Ligand-independent role of ErbB3 in endocytic recycling

Ana Rosa Saez-Ibanez[1,2], Julia M. Scheffler[1,3#], Takeshi Terabayashi[1,4#], Olof Idevall[5], Ingvar Ferby[1,2*]

[1] Ludwig Institute for Cancer Research, Science for Life Laboratory, Uppsala, Sweden

[2] Department of Medical Biochemistry and Microbiology, Science for Life Laboratory, Uppsala University, Uppsala, Sweden

[3] Current address: Department of Rheumatology and Inflammation Research, Gothenburg University, Gothenburg, Sweden

[4] Current address: Department of Pharmacology, Oita University, Faculty of Medicine, Oita, Japan

[5] Department of Medical Cell Biology, Uppsala University, Uppsala, Sweden

[#]these authors contributed equally

*To whom correspondence should be addressed: Ingvar Ferby, e-mail:ingvar.ferby@imbim.uu.se

Running title: *Integral role of ErbB3 in the endocytic recycling machinery*

Key words:

ErbB3, endocytic recycling, integrin β1, rabaptin-5, GGA3, Rab4, endosome

Abstract

Internalisation and trafficking of activated receptor tyrosine kinases (RTKs) determines duration and spatial distribution of growth factor signalling. Here we show that the ErbB3 receptor, frequently overexpressed in invasive cancers, acts in a ligand-independent manner to sort cargo such as β1 integrins and the transferrin receptor (TfR) for endocytic recycling breast epithelial cells. Loss of ErbB3 abrogates recycling of β1 integrins from a Rab4-positive compartment and redirects it towards degradation. Consequently, delivery of β1 integrins to the leading front of migrating epithelial cells is impaired and cell migration compromised upon loss of ErbB3. Mechanistically, ErbB3 interacts with and stabilises the Rab4/5 effector rabaptin5 and the endosomal adaptor GGA3 thereby facilitating assembly of the Arf6-GGA3-rabaptin5 complex, required for recycling of cargo including integrins and TfR. We here show that ErbB3 is an integral part in the endosomal trafficking machinery, provoking the notion that RTKs might play a more instrumental role in vesicular trafficking than commonly perceived.

Introduction

The Epidermal growth factor receptor (EGFR) family of receptor tyrosine kinases (RTKs), including EGFR, ErbB2, ErbB3 and ErbB4, form homo- or heterodimers and play key roles in epithelial development and homeostasis while their deregulation contributes to most epithelial cancers[1]. Upon ligand-binding the RTK dimers are activated, leading to recruitment of signalling molecules that initiate intracellular signalling cascades. ErbB3 has limited kinase activity but growing evidence highlight its potent oncogenic activity. In particular, ErbB3 has been linked to the migratory behaviour and metastasis of cancer cells[2–5]. ErbB3 is also responsible for acquired resistance to anti-EGFR and -ErbB2 therapies, and thus an intensely pursued therapeutic target (reviewed[6]).

Ligand-binding to RTKs triggers receptor internalisation and trafficking within the cells which determines strength, duration and spatial distribution of EGFR signals[7–11]. RTKs, including EGFRs are internalised through clathrin-dependent and -independent mechanisms, converging on the delivery of the receptors to early endosomes[7]. Thereafter, the receptors are either diverted towards protein degradation via late endosomes/lysosomes or recycled back to the plasma membrane. Recycling of RTKs or other transmembrane proteins to the cell surface can occur either directly from early endosomes

via a Rab4-dependent "short-loop" or via a Rab11-dependent "long-loop" endocytic recycling compartment[12].

Recently, the ubiquitously expressed GGA1 and GGA3 proteins, which are clathrin adaptors dependent on small GTPases of the Arf family, have been found to regulate Rab4-dependent endosomal recycling of β1 integrins (GGA3), transferrin receptor (GGA1) and Met RTK (GGA3)[13–17]. GGA proteins contain several functional domains that, for example, binds accessory proteins that modulate membrane trafficking such as rabaptin5[16,18,19]. Rabaptin5 and the closely related family member rabaptin4 are effectors of both Rab4 and Rab5[20–22]. Rabaptins promote fusion of vesicles to early endosomes and are additionally thought to cooperatively link Rab5- and Rab4-containing microdomains on early endosomes to coordinate the coupling between these domains[23] thereby regulating sorting of cargo including integrin β3 and TfR into recycling endosomes[24–26].

Here, we studied the role ErbB3 in vesicular trafficking and unexpectedly found that it constitutes an integral component of the endocytic recycling machinery that is required for recycling of β1 integrins and the TfR. ErbB3 associates with and promotes assembly of the Arf6-GGA3-rabaptin5 adaptor complex by stabilising the GGA3 and Rabaptin5 proteins.

Results

ErbB3 is required for endocytic recycling of β1 integrins and the transferrin receptor

ErbB3 is continuously endocytosed and recycled[27,27,28], independently of both ligand stimulation and other members of the EGFR family[27]. We therefore investigated if ErbB3 might regulate endocytic trafficking of cargo such as integrin β1, that also continuously internalise and recycle back to the plasma membrane to promote cell migration. To monitor endosomal trafficking of β1 integrins, the cell-surface pool of integrin β1 on mammary epithelial cells (MCF10A) was labelled with a fluorophore (Alexa488)-conjugated antibody on ice. Internalization was initiated by raising the temperature to 37°C, during which the integrins accumulate primarily in early endosomes[29]. The surface-labelling integrin antibody remaining on the cell surface was then quenched with an anti-Alexa488 antibody on ice, as previously described[13]. Cells were subsequently incubated at 37°C and the return of recycled internalized integrin back to the basal membrane was followed by TIRF live cell imaging (Fig. 1a,b). Alternatively, cells were fixed at different times and imaged by confocal microscopy (Fig. 1c,d). In control cells, a proportion of chased integrin was detected back on the plasma membrane already after 5 minutes (Fig. 1a,b). Depletion of ErbB3 by RNAi interference did not notably affect internalisation of surface-labelled integrin β1 as evident by confocal imaging (Fig. 1c,d, 0 min), but prevented its recycling back to the plasma membrane (Fig. 1a-d). The amount of chased β1 integrin declined rapidly in ErbB3-depleted cells (Fig. 1c,d), indicative of a rerouting of the cargo from recycling towards degradation. This is in

line with the findings that impaired recycling of integrin leads to its rerouting to the lysosomes[15,30]. Notably, total protein levels of integrin β1, as determined by immunoblotting, did not change significantly in the absence of ErbB3 (Fig. 1e), while quantitative PCR analysis showed a modest 1.7-fold increase in integrin β1 mRNA levels (Fig. 1f). This suggests that elevated *de-novo* synthesis of integrin β1 compensates for the higher rate of integrin turnover in ErbB3-silenced cells. Interestingly, the uncovered requirement for ErbB3 for integrin recycling is independent of ErbB3 ligand-induced cell signalling since the recycling assay was conducted in cell culture medium devoid of growth factors.

To address if ErbB3 regulates endocytic recycling in a cargo-specific or unspecific manner we explored if depletion of ErbB3 also influences trafficking of the transferrin receptor (TfR). The TfR has been extensively studied as an example of a cell surface receptor that undergoes continuous internalisation and effective recycling, with limited sorting to late endosomes and lysosomes[31]. Cell surface TfR was tagged with Alexa594-conjugated transferrin on ice for 30 minutes. Unbound labelled transferrin was washed away and cells incubated at 37°C in the presence of unlabelled transferrin for up to an hour. Cells were brought back on ice and subjected to low pH treatment to quench Alexa594 that had returned to the cell surface, followed by visualisation of chased transferrin retained in endosomes by fluorescence imaging (Fig. 1g). After 1 hour at 37°C, most labelled transferrin had recycled. By contrast, half of the chased transferrin was still retained in endosomes in cells treated with ErbB3 siRNA (Fig. 1g,h).

In order to address if ErbB3 specifically regulates the recycling pathway or if it plays a more general role in exocytic trafficking, we analysed the trafficking of ectopically expressed vesicular stomatitis virus, VSV-G-ts-GFP. This temperature sensitive form of VSV-G accumulates in the endoplasmic reticulum (ER) at 40°C. Upon shift to 32°C the protein traffics via the TGN and in a Rab11-dependent manner to the cell surface. We found that silencing of ErbB3 did not affect the rate by which VSV-G is transported from the ER to the cell surface as monitored by pull-down of surface biotinylated proteins (Supplemental Fig. 1).

Taken together, these results suggest a role for ErbB3 in promoting endocytic recycling of both β1 integrin and TfR in a manner that does not require ligand-stimulation of ErbB3.

ErbB3 is required for delivery of β1 integrins to the leading edge of migrating epithelial cell sheets

Endocytic recycling is important for polarised distribution of integrins in migrating cells[13,32–34] and integrin β1 localizes to the leading edge of migrating epithelial cells in a Rab4-dependent manner[13]. To test if ErbB3 regulates the distribution of newly recycled integrin β1 in sheets of migrating epithelia, a scratch was inflicted on confluent monolayers of MCF10A and incubated with surface labelling Alexa488-conjugated integrin β1 antibody for 1 hour on ice, prior to removal of the antibody and

subsequent incubation at 37°C for 1 hour. Chased integrin β1 and actin was visualised in cells at the leading front of the migrating cell sheet by immunofluorescence imaging (Fig. 2a). In control siRNA-transfected cells, surface integrin β1 localized at the leading front and along cell-cell contacts both prior to and after 1 hour tracing at 37°C (Fig. 2a). By contrast, in ErbB3-depleted cells, surface integrin β1 was only visible along cell-cell contacts but not at that leading front prior to the chase, while after 1 hour at 37°C, the level of chased integrin β1 diminished markedly (Fig. 2a). This result suggests that ErbB3 is required for recycling of β1 integrins back to the cell surface and that impaired recycling instead causes integrin degradation.

Given that recycling of β1 integrins is critical for cell migration one would predict that loss of ErbB3 impairs cell motility. We therefore subjected control or ErbB3 siRNA-transfected MCF10A cells to a scratch "wound healing" assay (Fig. 2b,c). siRNA-depletion of ErbB3 reduced the rate of scratch closure by about half compared to control cells. The assay was performed in the presence of the dual EGFR/ErbB2 specificity inhibitor lapatinib, in order to eliminate influence of canonical EGFR/ErbB2 signalling known to promote cell migration[35,36]. Thus, ErbB3 can promote cell migration independently of transphosphorylation by EGFR or ErbB2.

Loss of ErbB3 causes lysosomal degradation of internalised β1 integrins

Our experiments chasing the fate of surface-labelled integrin β1 indicate that loss of ErbB3 prevents recycling of endocytosed integrin and directs it towards degradation. In order to directly assess the impact of ErbB3 on integrin β1 stability, we subjected control or ErbB3 siRNA-transfected cells to treatment with the protein synthesis inhibitor cycloheximide and monitored integrin β1 levels by western blotting (Fig. 3a,b). While integrin β1 remained fairly stable in control cells for up to 8 hours of blocked protein synthesis, integrin levels gradually decreased in ErbB3-depleted cells (Fig. 3a,b). To complement the cycloheximide data, we performed a pulse-chase analysis of integrin β1 turnover. Control or ErbB3 siRNA-transfected MCF10A cells were labelled with ^{35}S-methionine/cysteine for 1 hour, followed by chasing with un-labelled amino acids at 37°C. Integrin β1 was subsequently immunoprecipitated and the retained ^{35}S-label determined by radiography. The data show that ErbB3-depleted cells exhibited accelerated integrin β1 turnover as compared with control-treated cells (Fig. 3c,d).

In order to determine if loss of ErbB3 promotes degradation of β1 integrins by the lysosomes, we next traced surface-labelled integrin β1 in control or ErbB3 siRNA-transfected MCF10A cells by confocal fluorescence microscopy, in the presence or absence of the lysosomal inhibitor chloroquine (Fig. 3e). Chloroquine treatment caused traced integrin β1 to accumulate in cells bordering the migratory front of scratched monolayer of both wild type and ErbB3-depleted cells. Quantification of fluorescence

intensity of traced integrin β1 showed that while levels are reduced by about 50% in the ErbB3-depleted cells, consistent with its increased protein turnover, chloroquine restored levels to those of wild type cells (Fig. 3f). This result demonstrates that elevated integrin β1 turnover caused by ErbB3-loss is due to increased lysosomal degradation.

ErbB3 and β1 integrins associate with Rab4-positive recycling endosomes

To investigate if ErbB3 and integrin β1 co-localize, we visualized their subcellular localisation by confocal microscopy. ErbB3 localised predominantly in intracellular vesicles in MCF10A cells (Fig. 4a). Surface-labelled integrin β1, that had been allowed to internalise for 30 minutes, co-localised only sporadically with ErbB3-mCherry. However, following a brief 10 minutes treatment with primaquine that blocks endocytic recycling, prominent co-localisation was observed (Fig. 4a), suggesting that ErbB3 and β1 integrins co-exist in recycling endosomes. To test if ErbB3 resides in recycling compartments, ErbB3-mCherry was co-expressed with either GFP-Rab4 or GFP-Rab11 in MCF7 cells followed by treatment with either primaquine or vehicle alone for 10 minutes and subsequent visualisation of the proteins by confocal imaging (Fig. 4b,c,d). Upon primaquine-treatment, ErbB3 associated extensively with Rab4-positive vesicles, while no co-localization was apparent between ErbB3 and Rab11-positive compartments. We also examined if ErbB3-mCherry localises in Rab5 or EEA1 positive early endosomes (Supplemental Fig. 2a,b). Limited perinuclear co-localization of ErbB3 and GFP-Rab5 could be observed, however, peripheral Rab5 or EEA positive vesicles did not co-localise with ErbB3. Taken together these results indicate that ErbB3 associates with β1 integrins on Rab4-positive fast recycling endosomes.

ErbB3 interacts with Rabaptin5 and GGA3 to promote their stability

We next explored whether or not ErbB3 physically interacts with β1 integrins or selected components of the machinery implicated in sorting β1 integrins for Rab4-dependent fast recycling, including Rab4, Rab5, the Rab4/5 effector rabaptin5, the adaptor protein GGA3 and the sorting nexin 17 (SNX17). Towards this end, we immunoprecipitated endogenous ErbB3 from MCF10A cell extracts and examined co-precipitating proteins by western blotting. While we did not detect co-immunoprecipitation of ErbB3 with integrin β1, Rab4, Rab5 or SNX17 (data not shown), we found that both GGA3 and rabaptin5 co-precipitated efficiently at the endogenous level (Fig. 5a). The interaction of ErbB3 with GGA3 or rabaptin5 increased after a 30-minute treatment with primaquine, consistent with them interacting in the recycling compartment. GGA3 has previously been shown to be required for Rab4-dependent recycling of β1 integrins, TfR and c-Met[14,15,17], while rabaptin5, which is an

accessory protein of GGA3, has been shown to regulate Rab4-dependent recycling of β3-integrins. GGA3 and rabaptin5 are therefore plausible molecular players in ErbB3-regulated endocytic recycling.

Next, we tested if rabaptin5 and ErbB3 can interact directly with one another *in vitro*. Recombinant GST-tagged ErbB3 was incubated overnight with purified MBP-tagged rabaptin5, after which ErbB3 was pulled down with glutathione-beads and bound rabaptin5 assessed by immunoblotting. The data shows that rabaptin5 bound to ErbB3 *in vitro,* indicating that their interaction is direct (Fig. 5b). The direct interaction between ErbB3 and rabaptin5 raises the question of whether or not ErbB3 also regulates the function of rabaptin5. Rabaptin5 is an effector and binding partner of both Rab4 and Rab5 that in addition recruits Rabex5, the GDF/GTP exchange factor of Rab5. To determine if ErbB3 regulates the interaction of rabaptin5 with its effectors, we immuno-precipitated rabaptin5 from control or ErbB3 siRNA-transfected MCF10A cells and assessed bound proteins by western blotting. Loss of ErbB3 did, however, not influence the ability of rabaptin5 to bind Rab4, Rab5 or Rabex5 (data not shown).

In order to gain further evidence that ErbB3 and rabaptin5 associate in endocytic compartments we examined their localization in MCF10A cells by confocal microscopy (Fig. 5c). The data shows that Citrine-tagged ErbB3 and mCherry-tagged rabaptin5 partially co-localized in intracellular vesicles (Fig. 5c, upper panels), while they accumulated together in vesicles upon 30 minutes of treatment with primaquine (Fig. 5c, lower panels).

Western blot examination revealed that rabaptin5 and GGA3 protein levels were significantly reduced upon siRNA-silencing of ErbB3, both in the presence or absence of primaquine (Fig. 5d,e). This appears to be due to reduced protein stability rather than reduced gene transcription, since depletion of ErbB3 resulted in a modest increase in mRNA levels of rabaptin5 and GGA3 (Fig. 5e). In agreement, depletion of ErbB3 accelerated the turnover of GGA3 and rabaptin5 under conditions when de-novo protein synthesis was inhibited with cycloheximide (Fig. 5f). The reduced levels of GGA3 and rabaptin5 observed in ErbB3-depleted cells were rescued by treatment with the proteasome inhibitor MG132 but not the lysosome inhibitor chloroquine (Fig. 5g). This result suggests that loss of ErbB3 promotes proteasomal degradation of GGA3 and Rabaptin5.

Assembly of the GGA3 adaptor complex on endosomes depends on the small GTPase Arf6 that binds to the GAT domain of GGA3. We therefore investigated if the reduced stability of GGA3 and its accessory protein rabaptin5, observed upon loss of ErbB3, results in impaired assembly of the Arf6-GGA3-rabaptin5 complex. MCF10A cells were transfected with control or ErbB3 siRNA, prior to treatment with primaquine or vehicle alone for 10 minutes. Harvested cell lysates were subsequently subjected to immunoprecipitation of Arf6 and western blotting for bound GGA3 and rabaptin5 (Fig. 5h). The result shows that loss of ErbB3 indeed reduced the amount of GGA3 and rabaptin5 associated with Arf6 both in the presence or absence of primaquine.

Taken together, our data support the notion that ErbB3 promotes Rab4-dependent endocytic recycling of β1 integrins and TfR by promoting assembly of the Arf6-GGA3-rabaptin5 adaptor complex, by stabilising the GGA3 and rabaptin5 proteins.

Rabaptin5 is critical for recycling of β1 integrins

Although previous studies clearly demonstrated the critical importance of rabaptin5 for directing β3 integrins towards Rab4-dependent recycling, the same has not yet been demonstrated for β1 integrins. We therefore traced surface-labelled β1 integrins in MCF10A cells transfected with either control or rabaptin5 siRNA by confocal imaging. The result indicated that loss of rabaptin5 directed internalised β1 integrins to degradation, similar to loss of ErbB3 (Fig. 6a, b).

Furthermore, we examined the impact of rabaptin5 on integrin β1 stability by pulse-chase analysis of protein turnover. Control or rabaptin5 siRNA-transfected MCF10A cells were labelled with ^{35}S-methionine/cysteine for 1 hour, followed by chasing with un-labelled amino acids at 37ºC. Integrin β1 was subsequently immunoprecipitated and retained ^{35}S-label was determined by autoradiography. The data shows that rabaptin5-depleted cells exhibited accelerated integrin β1 turnover as compared with control-treated cells (Fig. 6c,d). Previous work has shown that siRNA-mediated silencing of GGA3 similarly re-routes β1 integrins from Rab4-dependent recycling towards lysosomal degradation[15]. Thus, loss of rabaptin5 or GGA3 mimics the effect of loss of ErbB3 on endocytic sorting of β1 integrins, supporting the hypothesis that ErbB3 regulates endosomal trafficking by stabilising GGA3 and rabaptin5.

Discussion

In this paper we report that the RTK ErbB3 acts in a ligand-independent manner to promote fast endocytic recycling of both β1 integrins and the transferrin receptor. Endocytic trafficking of RTKs provides critical spatial and temporal control of the intracellular signalling events they trigger, which ultimately governs cellular response. Hence, the mechanisms by which RTKs internalise and traffic within the cell has been subject to intense scrutiny. While prevailing knowledge centers on RTKs as vesicular passengers, our study provides a compelling example of an RTK playing an integral role in the endocytic trafficking machinery per se.

RTK signalling is integrated at many levels with the regulation of endocytic trafficking of, most notably, integrins[37–39]. Growth factor mediated activation of Akt or protein kinase D (PKD) can for

example regulate recycling of integrins by phosphorylating proteins, such as ACAP1, an ARF6GAP[40], or Rabaptin5[25], respectively. Conversely, several studies have shown that integrins alter recycling of other receptors, such as EGFR[41] and vascular endothelial growth factor receptor (VEGFR2)[42], further highlighting the close coordination of trafficking of integrins and RTKs. We find that ErbB3 can promote endocytic recycling of β1 integrins and TfR, and cell migration, independently of growth factor induced RTK signalling, thus under conditions when Akt and PKD activities are suppressed, suggesting that canonical ErbB3-driven tyrosine kinase signalling does not play a role. Intriguingly, EGFR has been reported to function in a ligand-independent manner to scaffold an exocyst subcomplex needed to assemble autophagosomes[43], inviting wider speculation that 'inactive' RTKs, as exemplified by EGFR and ErbB3, might play a more instrumental role in intracellular vesicular trafficking than commonly perceived.

We show that ErbB3 interacts with and stabilises GGA3 and rabaptin5 to promote assembly of the Arf6-GGA3-rabaptin5 clathrin-binding adaptor complex. GGA3 has previously been reported to be required to sort multiple cargos, such as β1 integrins, TfR, c-Met and major histocompatibility complex (MHC), for Rab4-dependent recycling[14,15,17]. It is therefore possible that ErbB3 drives recycling of not only β1 integrins and TfR, but all cargo that depends on Arf6-GGA3, although this remains to be thoroughly addressed. Furthermore, loss of ErbB3 redirects β1 integrins to lysosomes for subsequent degradation. This observation resembles the outcome of GGA3-depletion that also redirects both β1 integrin[15] and c-Met towards lysosomal degradation[14], or rabaptin5 depletion that we find similarly causes trafficking of internalised β1 integrin towards lysosome degradation. These results support the conclusion that ErbB3 drives endocytic recycling by stabilising GGA3 and rabaptin5, thereby facilitating assembly of the Arf6-GGA3-rabaptin5 vesicular adaptor complex.

Previous studies have found that β1 integrins can physically interact with EGFR and traffic together[41,44]. We did not find that depletion of ErbB3 influences internalisation of β1 integrins, nor did we observe any noticeable co-localisation of ErbB3 with Rab5-positive compartments. It is therefore possible that ErbB3 encounters β1 integrins first in early/sorting endosomes, presumably at the step when the cargo is sorted into Rab4-positive vesicles through engagement of the Arf6-GGA3-rabaptin5-complex. This possibility is supported by the observation that integrin β1 and ErbB3 co-localisation primarily occured upon treatment with the recycling inhibitor primaquine, when ErbB3 was retained in a Rab4-positive compartment. This coincided with binding of ErbB3 to GGA3 and rabaptin5, which we found also to be enhanced upon treatment with primaquine, in line with previous work showing that GGA3 is enriched in Rab4-, and to a much lesser extent Rab5-positive early endosomes and co-localised with endocytosed Met in these endosomes[14].

Given the indication that ErbB3 encounters cargo destined for recycling first in early/sorting endosomes, one would predict that a pool of ErbB3 resides in the sorting compartment at all times, awaiting arrival of cargo. In line with this prediction, ErbB3 has been found to continuously endocytose

and recycle back to the plasma membrane[27,28,45] independent of both ligand stimulation and other members of the EGFR family[45]. Notably, a unique feature of ErbB3 is that its steady-state level is, in contrast to EGFR or ErbB2, tightly controlled by ligand-independent ubiquitination by the E3-ligase Nrdp1 and subsequent proteasomal degradation[46,47]. It will be interesting to address if this additional level of regulation of ErbB3 abundance is important to control steady-state availability of ErbB3 within endosomal compartments.

Our data shows that ErbB3 is required for delivery of β1 integrins to the leading edge of migrating sheets of epithelial cells and subsequently cell migration. Several studies have established that recycling of integrin promotes cell migration and cancer cell invasiveness[48,49], although retrograde transport of internalised β1 integrins via the TGN and back to the plasma membrane has also been reported to be important. Our data showing that loss of ErbB3 did not interfere with trafficking of VSV-G from the TGN to plasma membrane indicates that integrin trafficking via the TGN does not involve ErbB3. It will be interesting to investigate if ErbB3, that is frequently overexpressed in metastatic cancers, could contribute to cancer dissemination in part by driving integrin recycling.

Methods

Cell lines and cell culture. MCF10A cells were cultured in DMEM/F12 (Gibco) supplemented with glutamine (Sigma-Aldrich), 5% horse serum (Gibco), 20 ng/ml epidermal growth factor (EGF) (Miltenyi Biotech), 0.5 mg/ml hydrocortisone, 100 ng ml^{-1} cholera toxin and 10 μg/ml insulin (all from Sigma-Aldrich). Where indicated, a starvation medium lacking serum, insulin and EGF was used. MCF7 cells were cultured in EMEM supplemented with 0.01 mg/ml human recombinant insulin and 10% fetal bovine serum. HeLa cells were cultured in DMEM (Sigma-Aldrich) with 10% FBS (Gibco). All cell lines were purchased from ATCC. Culture conditions were 5% CO2 at 37 °C. For immunocytochemistry coverslips were coated with type I bovine collagen solution (Advanced BioMatrix) in 1:1000 in 0.02 M acetic acid overnight prior to application of cells.

Antibodies. The following primary antibodies were used: anti-ErbB3 (clone 2F12; Upstate Cell Signaling Solutions) for IP; anti-ErbB3 (clone D22C5; Cell Signaling) for western blotting; anti-integrin β1 (monoclonal, ab52971 from Abcam); anti-Rabex-5 (monoclonal, sc-166049 from Santa Cruz Biotechnology); anti-Rabaptin5 (monoclonal, sc-271069 from Santa Cruz Biotechnology); anti-GGA3 (clone 8; BD Transduction Laboratories); anti-SNX17 (10275-1AP, Proteintech); anti-Arf6 (clone 3A-1, Santa Cruz Biotech.); anti-GAPDH (clone 14C10; Cell Signaling); anti-α-tubulin (clone T5168, Sigma-Aldrich). For western blotting HRP-conjugated goat anti-mouse or goat anti-rabbit (The Jackson Laboratory) secondary antibodies were used. Alexa fluor® 594 or Alexa fluor® 488-conjugated anti-rabbit antibodies (The Jackson Laboratory) were used for immunocytochemistry. For the integrin recycling assay, Alexa Fluor® 488 anti-human integrin β1 antibody (clone TS2/16, Biolegend) was used.

SiRNA transfection. Cells were transfected with RNAiMAX (Invitrogen) according to supplier's instructions. A final concentration of 20 nM of siRNA was used. The following siRNAs were used: ErbB3 siRNA (5'CAAUACCAGACACUGUACAAGCUCU53' from Invitrogen), rabaptin5 siRNA (5'CCGGGCAAUUCUGAAUGAUACUAAA3' from Invitrogen) and scramble siRNA (non-targeting pre-designed ID 12935112, also from Invitrogen). The silencing experiments were performed 48 h post transfection.

Drugs and inhibitors. The EGFR/ErbB2 inhibitor lapatinib was used at 1 μM (LC Laboratories); cycloheximide at 50 μM (from Sigma-Aldrich), chloroquine at 50 μM (#14774 from Cell Signaling). In all three cases, control cells were treated with vehicle alone (DMSO, from Sigma-Aldrich) at the corresponding concentration. Primaquine was used at 0.5 mM (#160393 from Sigma-Aldrich) for 10 or 30 minutes.

Plasmids and DNA transfection. MCF10A cells were transfected with Lipofectamine 3000 (Invitrogen) according to supplier's instructions. Constructs for Rab4, Rab5, Rab11 and Rabaptin5 were kindly provided from Marino Zerial (MPG Dresden, Germany), and mCherry- och Citrine-tagged ErbB3 were kindly provided by Martin Offterdinger (Innsbruck, Austria). Rabaptin5 was subcloned into pMALC2 for bacterial expression.

qPCR analysis. RNA was extracted with RNeasy Mini Kit (#74104 from Qiagen). cDNA was synthesized with iScript™ cDNA Synthesis Kit (#170-8891 from Bio-Rad). qPCR was performed using KAPA SYBR® Fast and primers for ITGB1 (5'AGATCCGAAGTTTCAAGGGC3' and 5'GAACCATGACCTCGTTGTTC3'), GGA3 (5'GGGACAGGGTGTGAGAAAG3' and 5'AGAGGGGATCAGCGTCCTAT3'), RABEP1 (5'TTCCCAGCCTGACGTTTCTC3' and 5'GCTGCTGTTGTGCACGTAAA3') and GAPDH (5'CCCTTCATTGACCTCAACTA3' and 5'CCAAAGTTGTCATGGATGAC3'). The comparative Ct method was used to calculate fold change in gene expression in respect to GAPDH.

Western blotting. Cells were lysed in sodium dodecyl sulphate (SDS)-sample buffer (120 mM Tris-HCl pH 6.8, 3 % SDS, 15 % glycerol, 0.03 % bromophenol blue, 75 mM dithiothreitol (DTT) and run on 8-10% polyacrylamide gels. Proteins were transferred onto Hybond™-P polyvinylidene fluoride (PVDF) membranes at 100 V for 120 min at 4°C. Membranes were blocked in 4% milk or 5% bovine serum albumin (BSA), dissolved in TTBS (tris-buffered saline, 0.1% Tween 20). The protein bands were visualised using ECL™ or ECL plus™ reagents and Hyperfilm® ECL (all from GE Healthcare) and detected with a CCD camera (Biorad). Quantification of western blots was performed with ImageJ software.

Immunoprecipitation. Cells were lysed in 1% Triton X-100 buffer supplemented with Halt™ phosphatase/protease inhibitor (ThermoFisher). Preclearing was performed by incubating samples

for 1 h at 4°C under rotation with Pierce™ control agarose resin. Antibody incubation was performed overnight. Precipitated proteins were resolved by western blotting.

Immunocytochemistry. MCF10A cells cultured on uncoated coverslips were fixed with 4% PFA in PBS for 20 min, permeabilized with 0.5% Triton in PBS for 10 min and then blocked in Superblock T20 blocking buffer (Thermo Scientific). Primary and secondary antibodies and, where indicated, Alexa fluor® 488-conjugated Phalloidin (Life Technologies) were diluted in blocking buffer. Coverslips were mounted using ProLong® Antifade Reagent (Life Technologies) with or without DAPI. Images were taken with a Leica SP8 (confocal) or Zeiss Axio Imager M2 (epifluorescence) microscopes and processed using Leica Suite or Zeiss ZEN 2011 software, respectively.

Integrin recycling assay. MCF10A cells were plated on collagen-coated 24-well plates either sparsely or at high confluency for subsequent scratching. Cells were growth factor deprived for 3 h and then put on ice for 5 minutes to cool down. Surface integrin β1 was labelled at 4°C during 45 minutes, then washed twice with PBS and returned to 37°C in order to allow internalisation. After 15 minutes, cells were put back on ice and treated for 1h with anti-Alexa fluor® 488 (#A11094 from Life Technologies) in order to quench remaining surface signal. After quenching, cells were again washed twice with PBS and incubated in deprivation media at 37°C. At indicated times (0, 15, 30 or 60 minutes) cells were fixed with PFA 4% in PBS for 20 minutes at room temperature. When only integrin internalisation was monitored, the quenching step was not performed. Quantification (figure 1d) was performed for one of three representative experiments. Total pixel intensity per cell (n=6-8 per data point) was determined with ImageJ. Quantification (figure 3f) was performed for one of three representative experiment: Mean pixel intensity of 12-15 cells bordering the scratch from 4 separate areas along the scratches was determined with ImageJ.

TIRF microscopy. A prism-type TIRF microscope built around a Nikon E600FN upright microscope equipped with a 16X 0.8-NA water-immersion objective was used. The output from diode-pumped solid-state lasers (Cobolt, Stockholm, Sweden) were merged by dichroic mirrors and homogenized and expanded by a rotating, light-shaping diffusor (Physical Optics Corp., Torrance, CA). Excitation light was selected by interference filters (491 nm for Alexa-488 and 561 nm for mRFP, Chroma) mounted in a filter wheel (Lambda 10-3, Sutter Instruments, Novato, CA) and refocused through a modified dove prism (Axicon, Minsk, Belarus) at a 70° angle to achieve total internal reflection. Cells grown on 25-mm glass coverslips (Menzel-Gläser, #1) were kept on ice and mounted in a modified Sykes-Moore perfusion chamber just before imaging, placed on top of the prism and perfused with DMEM+F12 at a rate of 0.1 mL/min. Emission wavelengths were selected with interference filters (525/25 nm for Alexa 488, 590/20 for mRFP, Chroma) mounter in a filter wheel (Sutter Instruments) and fluorescence was detected by a back-illuminated EM-CCD camera (DU-887, Andor Technology, Belfast, Northern Ireland). Filter wheels and camera were controlled by MetaFluor (Molecular Devices Corp.,

Downington, PA) and images were acquired every 10 s. An electronic shutter prevented light exposure between image captures. Imaging was done at 37°C.

TIRF microscopy images were analysed off-line using ImageJ. Briefly, cell footprints were manually identified and regions of interest covering the edges of the adherent cells were draw. Intensity changes within these regions through the time course of the experiment (45 min) were measured and exported to Excel. All data points were background corrected, followed by normalization to the pre-stimulatory level (F/F0). Cells within large cell clusters were excluded from the analysis.

Transferrin recycling assay. Cells were incubated in starvation media supplemented with 25 mM HEPES for 3 h prior to the assay. Cells were treated with 5 µg/mL of Alexa fluor®-conjugated transferrin (T13343, from ThermoFisher) for 30 minutes on ice. Thereafter, excess of labelled transferrin was removed by three washes with PBS and subsequently incubated in media containing 50 µg/ml holo-transferrin (T4132, from Sigma-Aldrich) for indicated times (0, 5, 10, 15, 30, 60 minutes). Finally, the cells were treated with an acidic solution (0.2 M acetic acid and 0.5 M NaCl) for 30 seconds to remove surface labelling, fixed in 4% PFA in PBS for 20 minutes at room temperature and mounted. Quantification performed on one representative experiment from three replicates. Mean cell intensity was measured with ImageJ (n=6 images of 1-4 cells for each data point).

Wound healing assay. MCF10A cells were seeded in Falcon Multiwell 48-well plates and grown to full confluency. Before performing the wound, cells were pre-treated with lapatinib 1 µM. After 1 h, a scratch was placed in the middle of each well with a sterile pipette tip. After two washes with PBS, lapatinib-containing media was added back to the cells and the wound healing process was monitored using an IncuCyte ZOOM 40008 microscope for 14 h. The obtained images were analysed using the TScratch software. Quantification was performed on one of three representative experiments (n=2 wells). Wound closure was analysed with TScratch software.

^{35}S-Met/Cys pulse-chase protein turnover assay. MCF10A cells transfected with control or ErbB3 siRNA were incubated with growth factor deprived DMEM media lacking methionine and cysteine supplemented with 10 µCi/ml ^{35}S-methionine/cysteine (Perkin Elmer) for 30 minutes at 37°C. The labelling media was replaced with growth factor deprived MCF10A culture media containing 5 mM L-cysteine and 5 mM L-methionine (Sigma) for indicated times, prior to cell lysis and immunoprecipitation of integrin β1, SDS-polyacrylamide (PAGE) gel electrophoresis and detection of incorporated radioactivity using a Phosphoimager. Images were scanned and quantification of three independent experiments was perform in ImageJ.

Recombinant protein purification and *in vitro* binding assay. pMalC2-rabaptin5 was transformed into the BL21S(DE3)pLysS bacterial strain (Invitrogen). Protein expression was induced with 0.3 mM IPTG for 2 hours at 37°C and recombinant MBP-rabaptin5 was purified with an amylose resin (New

England Biolabs) according to manufacturs instructions and dialysed against lysis buffer (20 mM Tris-HCl ph7.4, 50 mM NaCl, 0.05 mM PMSF, 6 KIU7/ml aprotinin 0.5 mM DTT, 5% glycerol and 0.5% Triton X-100). Recombinant 6His-ErbB3 was purchased from Sigma. The in vitro binding assay was conducted by incubating 1 μg/ml recombinant ErbB3 with 1 μg/ml recombinant Rabaptin5 in a stringent buffer containing 50 mM Tris, pH 7.5, 150 mM NaCl, 1% NP40, 0.5% sodium deoxycholate, 0.1% SDS, 1 mM EDTA, HALT protease and phosphatase inhibitor overnight at 4°C. ErbB3 was immunoprecipitated and bound rabaptin5 detected by western blotting.

Colocalization analysis. Single Rab4 or Rab11 positive structures were identified and 40x40 pixel squares were drawn with the structures in the center and saved as separate images. For each cell, a minimum of 15 structures were randomly selected and the intensity of the center (7-pixel diameter circle, a) and the adjacent volume (background, b) for each structure was determined using ImageJ. These regions were subsequently transferred to the other channel (ErbB3) and similar measurements were performed. The relative enrichment of ErbB3 at the Rab-positive structures was determined by the formula (a-b)/b . An average for each cell was determined, and a minimum of 16 cells was analyzed for each condition. Images shown in the paper are average projections of all structures from all cells analyzed. Statistical analysis was performed using unpaired, 2-tailed Student's t-test with the significance level set to $P<0.05$

VSV-G trafficking assay. VSV-G ts045-GFP was expressed in MCF10A cells for 24 hours. Cells were incubated at 40°C for 6 hours, which causes misfolding and trapping of VSV-G in the ER. The cells were then shifted to permissive temperature (32°C) for up to 1 hour, followed by incubation on ice with Sulfo-NHS-SS-Biotin (Thermo Scientific) to biotinylate all surface proteins. Cells were lysed in 1% Triton X-100 containing lysis buffer followed by pulldown with Streptavidin-agarose beads (Sigma) overnight and western blot analysis.

References

1. Schlessinger, J. Ligand-induced, receptor-mediated dimerization and activation of EGF receptor. *Cell* **110,** 669–672 (2002).
2. Tiwary, S. *et al.* ERBB3 is required for metastasis formation of melanoma cells. *Oncogenesis* **3,** e110 (2014).
3. Pradeep, S. *et al.* Hematogenous metastasis of ovarian cancer: rethinking mode of spread. *Cancer Cell* **26,** 77–91 (2014).
4. Smirnova, T. *et al.* Phosphoinositide 3-kinase signaling is critical for ErbB3-driven breast cancer cell motility and metastasis. *Oncogene* **31,** 706–715 (2012).
5. Yoshioka, T. *et al.* Significance of integrin αvβ5 and erbB3 in enhanced cell migration and liver metastasis of colon carcinomas stimulated by hepatocyte-derived heregulin. *Cancer Sci.* **101,** 2011–2018 (2010).
6. Gaborit, N., Lindzen, M. & Yarden, Y. Emerging anti-cancer antibodies and combination therapies targeting HER3/ERBB3. *Hum. Vaccines Immunother.* **12,** 576–592 (2016).
7. Sorkin, A. & Goh, L. K. Endocytosis and intracellular trafficking of ErbBs. *Exp. Cell Res.* **315,** 683–696 (2009).
8. Avraham, R. & Yarden, Y. Feedback regulation of EGFR signalling: decision making by early and delayed loops. *Nat. Rev. Mol. Cell Biol.* **12,** 104–117 (2011).
9. Miaczynska, M. & Bar-Sagi, D. Signaling endosomes: seeing is believing. *Curr. Opin. Cell Biol.* **22,** 535–540 (2010).
10. Al-Akhrass, H. *et al.* Sortilin limits EGFR signaling by promoting its internalization in lung cancer. *Nat. Commun.* **8,** 1182 (2017).
11. Wiley, H. S. Trafficking of the ErbB receptors and its influence on signaling. *Exp. Cell Res.* **284,** 78–88 (2003).
12. Tomas, A., Futter, C. E. & Eden, E. R. EGF receptor trafficking: consequences for signaling and cancer. *Trends Cell Biol.* **24,** 26–34 (2014).

13. Arjonen, A., Alanko, J., Veltel, S. & Ivaska, J. Distinct recycling of active and inactive β1 integrins. *Traffic Cph. Den.* **13,** 610–625 (2012).
14. Parachoniak, C. A., Luo, Y., Abella, J. V., Keen, J. H. & Park, M. GGA3 functions as a switch to promote Met receptor recycling, essential for sustained ERK and cell migration. *Dev. Cell* **20,** 751–763 (2011).
15. Ratcliffe, C. D. H., Sahgal, P., Parachoniak, C. A., Ivaska, J. & Park, M. Regulation of Cell Migration and β1 Integrin Trafficking by the Endosomal Adaptor GGA3. *Traffic Cph. Den.* **17,** 670–688 (2016).
16. Puertollano, R. & Bonifacino, J. S. Interactions of GGA3 with the ubiquitin sorting machinery. *Nat. Cell Biol.* **6,** 244–251 (2004).
17. Zhao, Y. & Keen, J. H. Gyrating clathrin: highly dynamic clathrin structures involved in rapid receptor recycling. *Traffic Cph. Den.* **9,** 2253–2264 (2008).
18. Zhu, G. *et al.* Structural basis of Rab5-Rabaptin5 interaction in endocytosis. *Nat. Struct. Mol. Biol.* **11,** 975–983 (2004).
19. Zhai, P. *et al.* The interaction of the human GGA1 GAT domain with rabaptin-5 is mediated by residues on its three-helix bundle. *Biochemistry (Mosc.)* **42,** 13901–13908 (2003).
20. Vitale, G. *et al.* Distinct Rab-binding domains mediate the interaction of Rabaptin-5 with GTP-bound Rab4 and Rab5. *EMBO J.* **17,** 1941–1951 (1998).
21. Stenmark, H., Vitale, G., Ullrich, O. & Zerial, M. Rabaptin-5 is a direct effector of the small GTPase Rab5 in endocytic membrane fusion. *Cell* **83,** 423–432 (1995).
22. Nagelkerken, B. *et al.* Rabaptin4, a novel effector of the small GTPase rab4a, is recruited to perinuclear recycling vesicles. *Biochem. J.* **346 Pt 3,** 593–601 (2000).
23. de Renzis, S., Sönnichsen, B. & Zerial, M. Divalent Rab effectors regulate the sub-compartmental organization and sorting of early endosomes. *Nat. Cell Biol.* **4,** 124–133 (2002).
24. Pagano, A., Crottet, P., Prescianotto-Baschong, C. & Spiess, M. In vitro formation of recycling vesicles from endosomes requires adaptor protein-1/clathrin and is regulated by rab4 and the connector rabaptin-5. *Mol. Biol. Cell* **15,** 4990–5000 (2004).

25. Christoforides, C., Rainero, E., Brown, K. K., Norman, J. C. & Toker, A. PKD controls αvβ3 integrin recycling and tumor cell invasive migration through its substrate Rabaptin-5. *Dev. Cell* **23,** 560–572 (2012).
26. Deneka, M. *et al.* Rabaptin-5alpha/rabaptin-4 serves as a linker between rab4 and gamma(1)-adaptin in membrane recycling from endosomes. *EMBO J.* **22,** 2645–2657 (2003).
27. Fosdahl, A. M. *et al.* ErbB3 interacts with Hrs and is sorted to lysosomes for degradation. *Biochim. Biophys. Acta* **1864,** 2241–2252 (2017).
28. Cao, Z., Wu, X., Yen, L., Sweeney, C. & Carraway, K. L. Neuregulin-induced ErbB3 downregulation is mediated by a protein stability cascade involving the E3 ubiquitin ligase Nrdp1. *Mol. Cell. Biol.* **27,** 2180–2188 (2007).
29. Roberts, M., Barry, S., Woods, A., van der Sluijs, P. & Norman, J. PDGF-regulated rab4-dependent recycling of alphavbeta3 integrin from early endosomes is necessary for cell adhesion and spreading. *Curr. Biol. CB* **11,** 1392–1402 (2001).
30. De Franceschi, N., Hamidi, H., Alanko, J., Sahgal, P. & Ivaska, J. Integrin traffic - the update. *J. Cell Sci.* **128,** 839–852 (2015).
31. Sönnichsen, B., De Renzis, S., Nielsen, E., Rietdorf, J. & Zerial, M. Distinct membrane domains on endosomes in the recycling pathway visualized by multicolor imaging of Rab4, Rab5, and Rab11. *J. Cell Biol.* **149,** 901–914 (2000).
32. White, D. P., Caswell, P. T. & Norman, J. C. alpha v beta3 and alpha5beta1 integrin recycling pathways dictate downstream Rho kinase signaling to regulate persistent cell migration. *J. Cell Biol.* **177,** 515–525 (2007).
33. Ivaska, J. *et al.* PKCepsilon-mediated phosphorylation of vimentin controls integrin recycling and motility. *EMBO J.* **24,** 3834–3845 (2005).
34. Powelka, A. M. *et al.* Stimulation-dependent recycling of integrin beta1 regulated by ARF6 and Rab11. *Traffic Cph. Den.* **5,** 20–36 (2004).
35. Lauand, C., Rezende-Teixeira, P., Cortez, B. A., Niero, E. L. de O. & Machado-Santelli, G. M. Independent of ErbB1 gene copy number, EGF stimulates migration but is not associated with cell proliferation in non-small cell lung cancer. *Cancer Cell Int.* **13,** 38 (2013).

36. Maretzky, T. *et al.* Migration of growth factor-stimulated epithelial and endothelial cells depends on EGFR transactivation by ADAM17. *Nat. Commun.* **2,** 229 (2011).
37. Ivaska, J. & Heino, J. Cooperation between integrins and growth factor receptors in signaling and endocytosis. *Annu. Rev. Cell Dev. Biol.* **27,** 291–320 (2011).
38. Woods, A. J., White, D. P., Caswell, P. T. & Norman, J. C. PKD1/PKCmu promotes alphavbeta3 integrin recycling and delivery to nascent focal adhesions. *EMBO J.* **23,** 2531–2543 (2004).
39. Caswell, P. T., Vadrevu, S. & Norman, J. C. Integrins: masters and slaves of endocytic transport. *Nat. Rev. Mol. Cell Biol.* **10,** 843–853 (2009).
40. Li, J. *et al.* Phosphorylation of ACAP1 by Akt regulates the stimulation-dependent recycling of integrin beta1 to control cell migration. *Dev. Cell* **9,** 663–673 (2005).
41. Caswell, P. T. *et al.* Rab-coupling protein coordinates recycling of alpha5beta1 integrin and EGFR1 to promote cell migration in 3D microenvironments. *J. Cell Biol.* **183,** 143–155 (2008).
42. Reynolds, A. R. *et al.* Stimulation of tumor growth and angiogenesis by low concentrations of RGD-mimetic integrin inhibitors. *Nat. Med.* **15,** 392–400 (2009).
43. Tan, X., Thapa, N., Sun, Y. & Anderson, R. A. A kinase-independent role for EGF receptor in autophagy initiation. *Cell* **160,** 145–160 (2015).
44. Yu, X., Miyamoto, S. & Mekada, E. Integrin alpha 2 beta 1-dependent EGF receptor activation at cell-cell contact sites. *J. Cell Sci.* **113 (Pt 12),** 2139–2147 (2000).
45. Sak, M. M. *et al.* The oncoprotein ErbB3 is endocytosed in the absence of added ligand in a clathrin-dependent manner. *Carcinogenesis* **33,** 1031–1039 (2012).
46. Diamonti, A. J. *et al.* An RBCC protein implicated in maintenance of steady-state neuregulin receptor levels. *Proc. Natl. Acad. Sci. U. S. A.* **99,** 2866–2871 (2002).
47. Qiu, X.-B. & Goldberg, A. L. Nrdp1/FLRF is a ubiquitin ligase promoting ubiquitination and degradation of the epidermal growth factor receptor family member, ErbB3. *Proc. Natl. Acad. Sci. U. S. A.* **99,** 14843–14848 (2002).
48. Caswell, P. T. *et al.* Rab-coupling protein coordinates recycling of alpha5beta1 integrin and EGFR1 to promote cell migration in 3D microenvironments. *J. Cell Biol.* **183,** 143–155 (2008).
49. Pellinen, T. & Ivaska, J. Integrin traffic. *J. Cell Sci.* **119,** 3723–3731 (2006).

Acknowledgments

We thank Taija Makinen for help with confocal microscopy, and Marino Zerial, Lukas Huber and Martin Offterdinger for kindly providing cDNA constructs. We also thank to Carl-Henrik Heldin and Staffan Johansson for valuable discussion and for critically reading the manuscript.

Author contributions

A.R.S., J.S, T.T. and I.F. conceived and designed the experiments. A.R.S, and J.S performed the experiments and A.R.S., J.S. and I.F. interpreted the results. A.R.S. and I.F. wrote the manuscript.

Figure legends

Figure 1: ErbB3 is required for endocytic recycling of β1 integrins and the transferrin receptor. **a** TIRF imaging of the basal membrane of live MCF10A cells after internalisation of Alexa488-labelled integrin β1. Note that ErbB3-depleted cells display defective integrin β1 recycling in comparison to the control cells. Experiment was performed in absence of growth factors. **b** Quantification of recycled integrin β1 determined as in (a). Values correspond to the normalized intensity of Alexa488 on three independent experiments. Number outside of brackets indicates the number of cells. **c** Immunofluorescence imaging of traced internalised integrin β1 and the membrane label CellMask (red). The MCF10A cells were transfected with control or ErbB3 siRNA and assay performed in growth factor deprived media. **d** Quantification of immunofluorescence intensity of internalised integrin β1 traced for indicated times (n=6-8 cells from one representative experiment). **e** Western blot analysis of ErbB3 and integrin β1 after transfection of MCF10A cells with control or ErbB3 siRNA. **f** Relative levels of ErbB3 mRNA in control or ErbB3 siRNA transfected cells as determined by quantitative PCR (n=6 independent experiments). **g** Confocal imaging of Alexa594-conjucated transferrin chased with unlabelled holo-transferrin for indicated times in MCF7 cells. Note that siRNA-mediated depletion of ErbB3 caused intracellular retention of transferrin. **h** Quantification of Alexa594 fluorescence intensity in cells treated as in **e** (n=6 frames of 1-4 cells for each data point from one representative experiment). **b,d,f,h** Data are presented as mean values ± s.e.m. *P≤0.05, **P≤0.01, ***P≤0.001 (two-tailed paired student's t-test). ns=non significant. Scale bar: 10 μm.

Figure 2: Ligand-independent role of ErbB3 in epithelial sheet migration. **a** Immunofluorescence imaging of surface-labelled integrin β1 (green) or actin (blue), 1 hour after scratching of confluent sheets of MCF10A cells (0 hr tracing), or after 1 hour incubation at 37°C (1 hour tracing). Note that depletion of ErbB3 abrogates integrin β1 localisation at the leading front. **b** Scratch closure assay of control or

ErbB3-depleted MCF10A cells, cultured in the presence of the EGFR/ErbB2 inhibitor lapatinib. **c** Quantification of scratch aperture of samples treated as in **b**. Data are presented as mean values ± s.e.m., n=2).

Figure 3: Loss of ErbB3 directs integrin β1 towards lysosomal degradation. **a** Western blotting of MCF10A cells, transfected with control or ErbB3 siRNA prior to treatment with the protein synthesis inhibitor cycloheximide (CHX) for indicated times. **b** Quantification of integrin levels at indicated times after CHX treatment, determined as in (**a**) (n=3 independent experiments). **c** Determination of integrin β1 turnover by pulse-chase metabolic labelling. Control or ErbB3 siRNA-transfected MCF10A cells were pulse-chase labelled with radioactive (^{35}S) methionine and cysteine. Radiolabelled integrin β was visualised by radiography of immunoprecipitates (upper panel). Cell lysates and immunoprecipitates were analysed by immunoblotting. **d** Quantification of pulse chased ^{35}S-labelled integrin β1, as in (**c**) (n=4 independent experiments). **e** Immunofluorescence imaging of surface-labelled integrin β1 (using an Alexa488-conjugated anti-integrin β1 antibody), prior to (0 hours) or after tracing at 37°C for 1.5 hours. A scratch was inflicted prior to antibody incubation. Note that application of the lysosome inhibitor chloroquine caused accumulation of integrin β1 in intracellular vesicular compartments both in control of ErbB3-depleted cells. **f** Quantification of integrin β1 fluorescence intensity in cells bordering the migratory front in samples treated as in **e**, showing that chloroquine restored total levels of integrin β1 in ErbB3-depleted cells. Data are presented as mean values ± s.e.m., (n=3).

Figure 4: ErbB3 co-localises with internalised integrin β1 and Rab4-positive vesicles. a Confocal imaging of ErbB3-mCherry and internalized surface-labelled integrin β1 (using an Alexa488-conjugated antibody). Cells (MCF10A) were treated with either primaquine or vehicle alone prior to imaging. **b** Confocal imaging of ErbB3-mCherry and indicated Rab marker, with or without primaquine (PQ). **c** Analysis of colocalization of ErbB3-mCherry and Rab4 or Rab11. Average projections of indicated number of GFP-Rab4 or GFP-Rab11 positive structures from 20 cells (3 independent experiments). **d** The relative enrichment of ErbB3 at the Rab-positive structures was determined by the formula (a-b)/b where a is the ErbB3-mCherry intensity of the center of Rab4 structures, and b the adjacent volume (background) for each structure. Each data point represent the average of a minimum of 20 structures in one cell. P-values were determined using unpaired, 2-tailed Student's t-test.

Figure 5: ErbB3 interacts with Rabaptin5 and GGA3 and promotes their stability. a Immunoblotting of ErbB3 immunoprecipitates or input cell lysates, following a 30 minute treatment with primaquine (PQ), showing endogenous binding of ErbB3 with GGA3 and rabaptin5 that increases upon PQ treatment. **b** *In vitro* binding of ErbB3 to rabaptin5. Western blotting of ErbB3-immunoprecipitates following incubation of recombinant ErbB3 and rabaptin5. **c** Confocal imaging of

ErbB3-Citrine and rabaptin5-Cherry expressed in MCF10A cells, with or without PQ. Note a prominent co-localisation after PQ treatment. Scale bar: 10 μm. **d** Western blotting of MCF10A cell lysates subjected to control of ErbB3 siRNA silencing, with or without treatment with PQ for 10 minutes. **e** Quantification of GGA3 and rabaptin5 protein levels (by western blotting) and mRNA levels (by quantitative PCR) in ErbB3 siRNA transfected MCF10A cells relative to control-transfected cells (n=4 for protein or n=3 for mRNA). Data are presented as mean values ± s.e.m. and P values (one sample student's t-test). Scale bar: 10 μm. **f** Western blotting analysis of MCF10A cells, transfected with control or ErbB3 siRNA prior to treatment with either protein synthesis inhibitor cycloheximide (CHX) for indicated times. **g** Western blotting analysis of MCF10A cells, transfected with control or ErbB3 siRNA prior to treatment with the proteasome inhibitor MG132 for indicated times. MG321 but not chloroquine restores GGA3 and rabaptin5 levels in ErbB3-depleted cells. **h** Immunoblotting of Arf6 immunoprecipitates or input cell lysates, following control of ErbB3 siRNA transfection and 10 minutes treatment with PQ or vehicle. Note that interaction of Arf6 with both GGA3 and rabaptin5 is reduced in the absence of ErbB3.

Figure 6: Loss of Rabaptin5 reduces integrin β1 recycling and promotes its degradation. a Confocal imaging of internalized surface-labelled integrin β1 (using an Alexa488-conjucated antibody), prior to (0 hours) or after tracing for 1 hour at 37°C. Cells were counter labelled with Alexa594-Phalloidin (actin) or DAPI (nuclei). **b** Quantification of integrin β1 fluorescence intensity of cells treated as in (**a**) (n=6, data are presented as mean values ± s.e.m.). *P≤0.05, **P≤0.01, (two-tailed paired student's t-test. **c** Determination of integrin β1 turnover by pulse-chase metabolic labelling. Control or rabaptin5 siRNA-transfected MCF10A cells were pulse-chase labelled with radioactive (^{35}S) methionine and cysteine. Radiolabelled integrin β1 was visualised by radiography of immunoprecipitates (upper panel). Cell lysates and immunoprecipitates were analysed by immunoblotting as indicated. **d** Quantification of radiolabelled integrin β1 at the indicated times of three independent pulse and chase experiments. Data are presented as mean values ± s.e.m. P values determined by two-tailed paired student's t-test.

Figure 7: ErbB3 drives endocytic recycling. Model illustrating that ErbB3 binds to and stabilises GGA3 and rabaptin5 to facilitate assembly of the Arf6-GGA3-rabaptin5 complex that is required to sort cargo, such as β1 integrins for Rab4-dependent recycling.

Supplementary Figure 1: ErbB3 does not regulate exocytic trafficking of VSVG from the ER. Western blot analysis of surface-biotinylated VSV-G-ts45-GFP, following its temperature-dependent release from the endoplasmic reticulum (ER) for indicated times. Note that ErbB3-depletion does not influence the emergence of VSVG at the plasma membrane.

Supplementary Figure 2: Limited co-localisation of ErbB3 with EEA1 positive vesicles. Confocal imaging of ErbB3-mCherry and GFP-Rab5 (**a**) or endogenous immunostained EEA1) in HeLa cells. Scale bar: 5 μm.

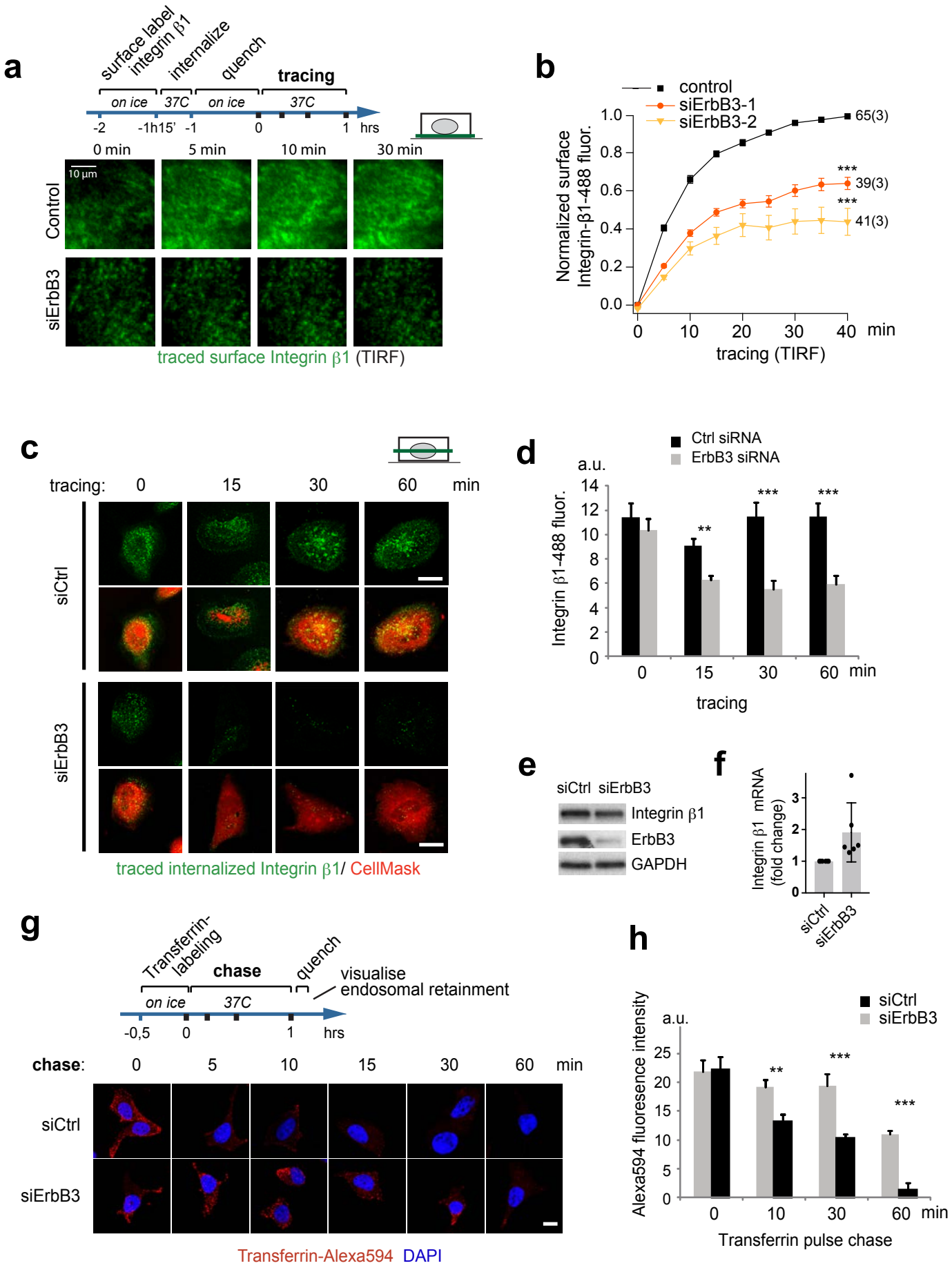

Saez et al., Figure 1

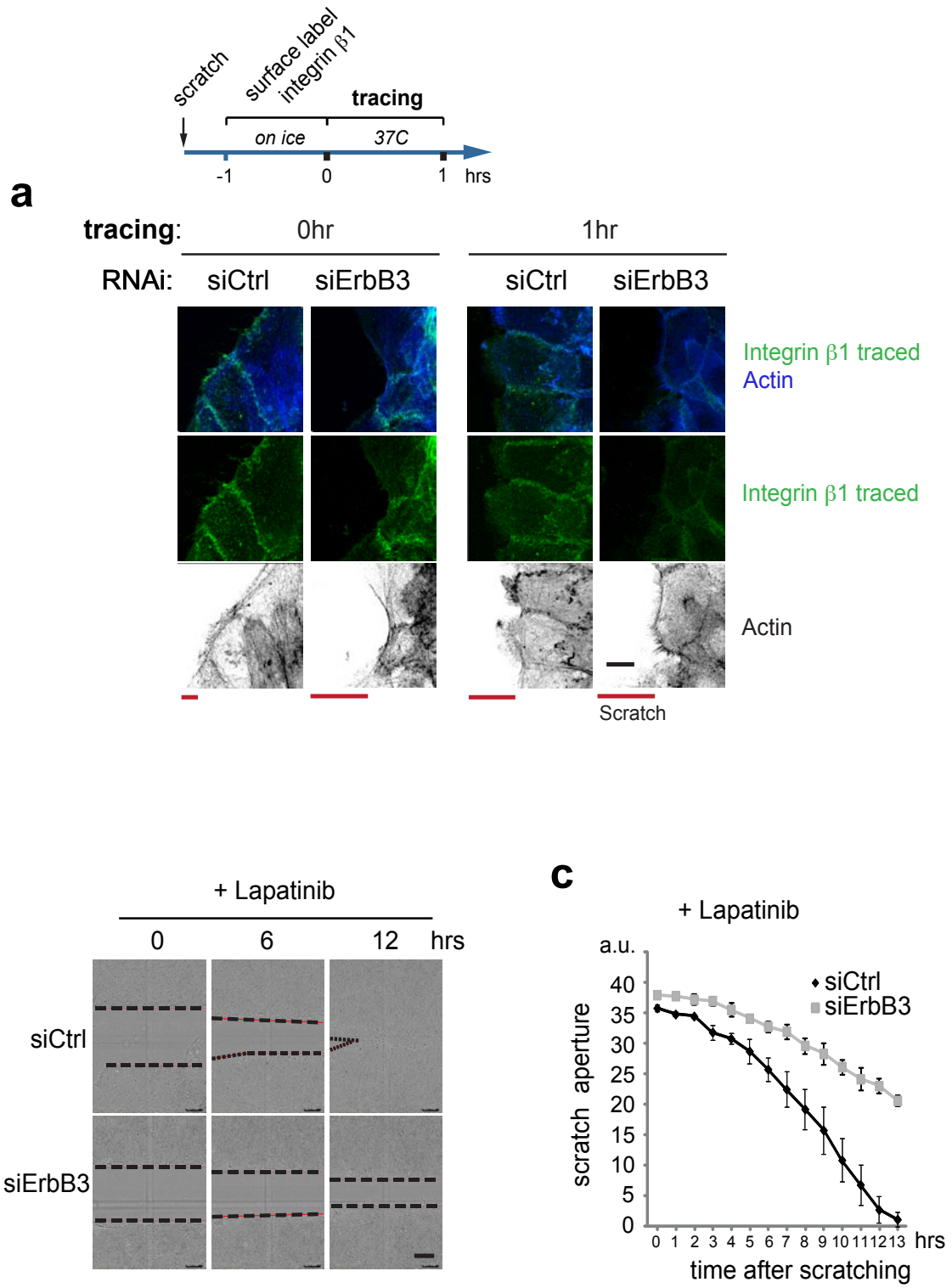

Saez et al., Figure 2

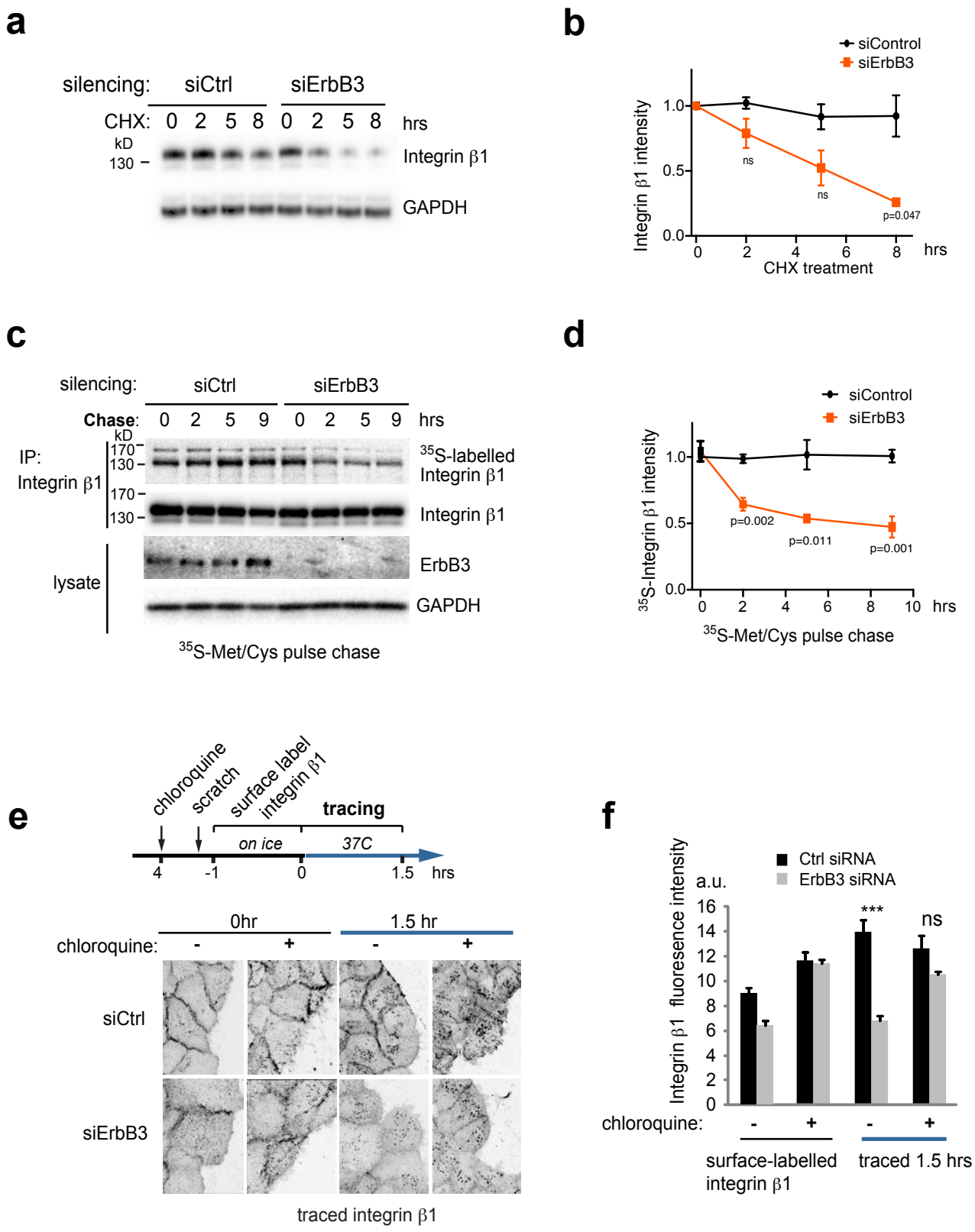

Saez et al., Figure 3

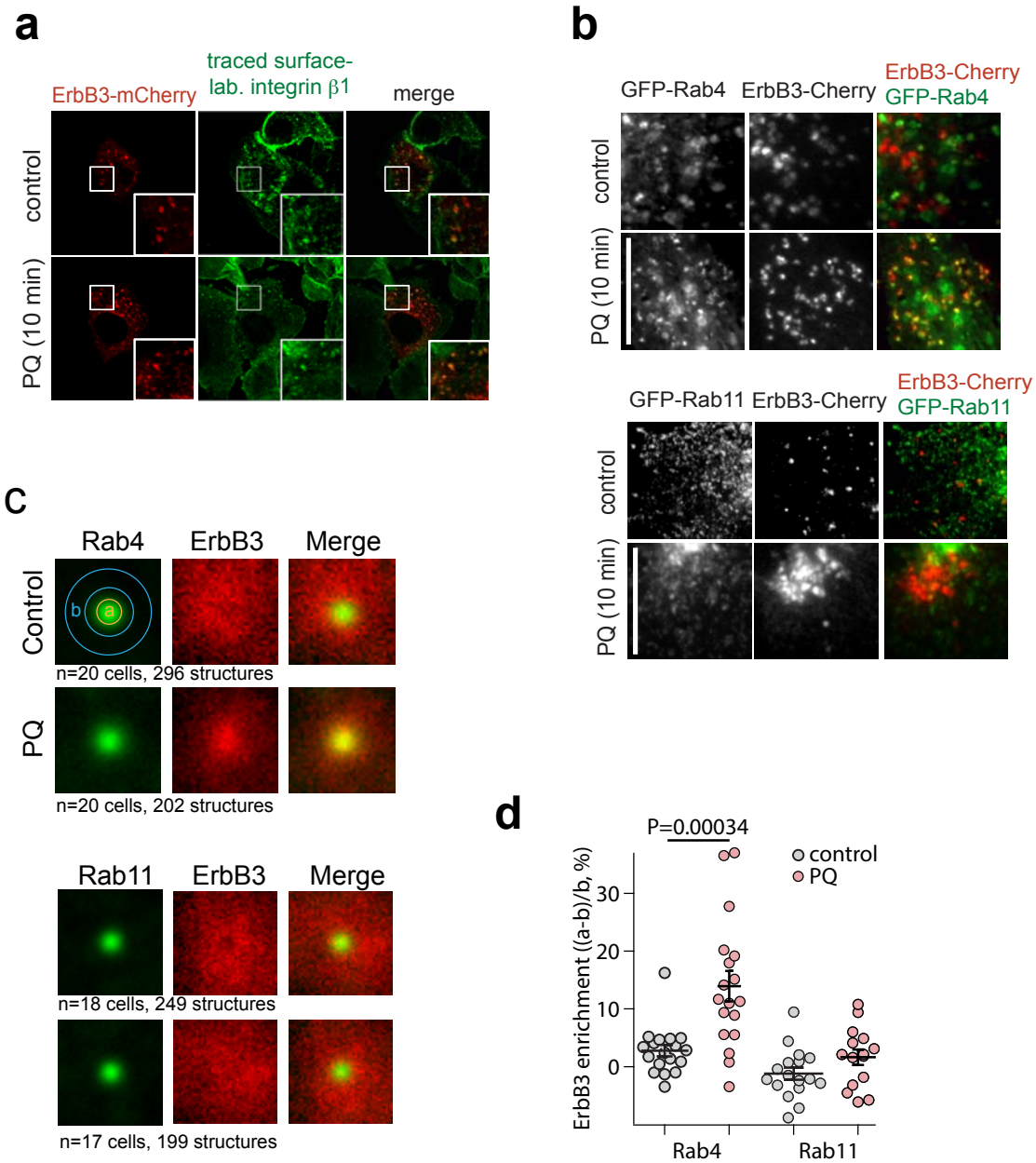

Saez et al., Figure 4

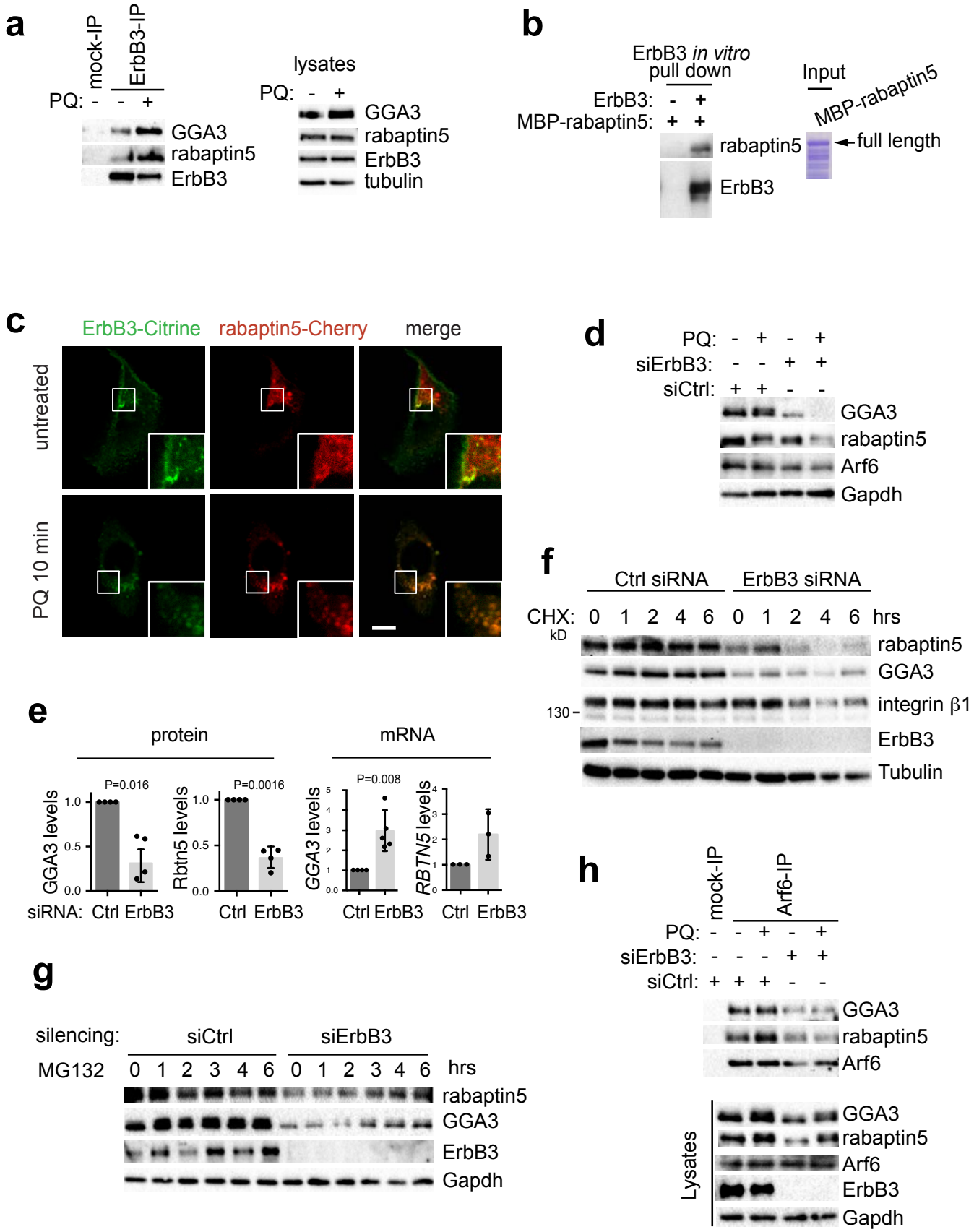

Saez et al., Figure 5

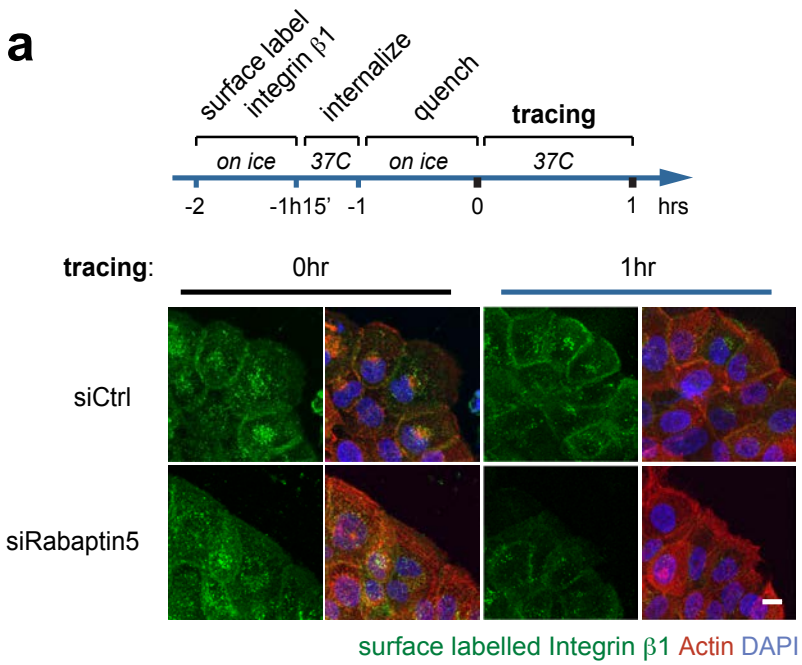

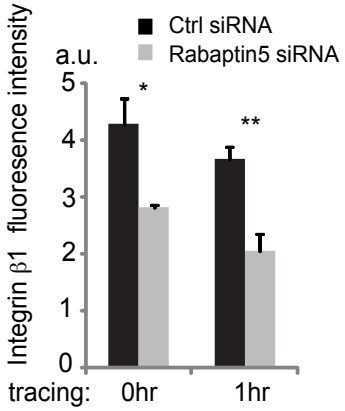

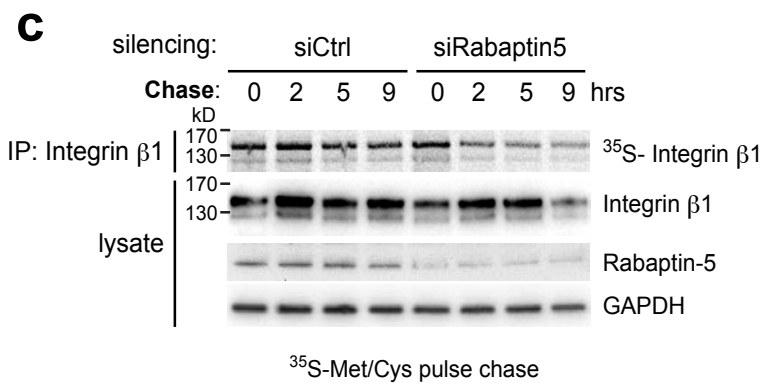

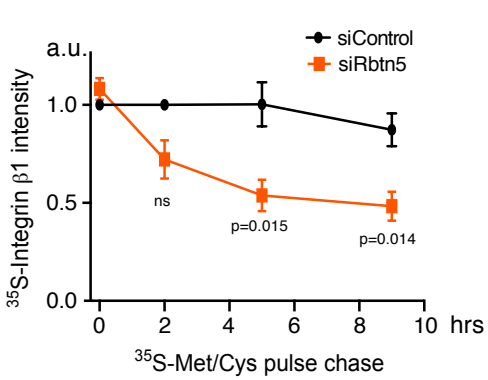

Saez et al., Figure 6